Effects of noise, correlations, and errors in the preparation of initial states in quantum simulations

Nayeli Zuniga-Hansen, Yu-Chieh Chi, and Mark S. Byrd
Physics Department and Computer Science Department, Southern Illinois University, Carbondale, Illinois 62901-4401, USA
(Received 12 March 2012; revised manuscript received 7 August 2012; published 25 October 2012)

In principle, a quantum system could be used to simulate another quantum system. The purpose of such a simulation would be to obtain information about problems which are difficult to simulate on a classical computer due to the exponential increase of the Hilbert space with the size of the system and which cannot be readily measured or controlled in an experiment. The system will interact with the surrounding environment and with the other particles in the system, and be implemented using imperfect controls, making it subject to noise. It has been suggested that noise does not need to be controlled to the same extent as it must be for general quantum computing. However, the effects of noise in quantum simulations are not well understood and how best to treat them in most cases is not known. In this paper we study an existing quantum algorithm for simulating the one-dimensional Fano-Anderson model using a liquid-state NMR device. We examine models of noise in the evolution using different initial states in the original model. We also add interacting spins to simulate a realistic situation where an environment of spins is present. We find that states which are entangled with their environment, and sometimes correlated but not necessarily entangled, have an evolution which is described by maps which are not completely positive. We discuss the conditions for this to occur and also the implications.

DOI: 10.1103/PhysRevA.86.042335 PACS number(s): 03.67.Lx, 03.65.Yz, 03.67.Ac

I. INTRODUCTION

Simulating quantum systems with quantum systems is one of the primary reasons there is a great deal of interest in building a quantum computing device. The difficulty of simulating quantum systems on a classical computer, mainly due to the exponential increase of the Hilbert space with system size, was Feynman's motivation for proposing the idea that a quantum system might perform this task much more efficiently [1]. Lloyd showed later that some quantum systems could be manipulated to represent the evolution of other quantum systems using only local interactions [2].

There are many problems of interest in quantum mechanics which have no known analytical solution. Thus for a wide range of physical systems simulation is a valuable tool for solving quantum-mechanical problems. Classical simulation of such systems can quickly become intractable as the number of particles increases. The resources required to perform such a task increase exponentially with the size of the system. For example, in order to represent the state of N two-state particles a 2^N vector is required and for its evolution the unitary operator will be a $2^N \times 2^N$ matrix [2,3]. However, a quantum simulator would require only N particles to simulate such a system [2,4]. In this sense, it is conjectured to provide exponential speedup over classical simulation [5], but that is not the only advantage; other problems such as the sign problem from quantum Monte Carlo algorithms for fermionic systems or the exchange-correlation functionals in density-functional theory [6,7], will not be present in a quantum simulation. Therefore, many difficult problems in particle physics, condensed matter systems, and quantum field theory and chemistry, among others, could be tackled [5,6,8–21].

Quantum simulations have received a great deal of recent attention, since they are feasible without the need for a universal quantum computing device. The question of the universality of Hamiltonians has been addressed to a great extent [22–31], and algorithms have been developed to simulate specific systems [4,6,12,19,32–43]. In addition, experiments have been designed and implemented [16,44–50]. Still, a great deal of work remains to be done. Currently available quantum simulating devices are built with relatively few controllable particles. These devices are, after all, quantum systems that inevitably interact with the surrounding environment and therefore are subject to noise. Just as with quantum computing, this is an important issue when it comes to scalability. It is therefore necessary to study how the interactions affect a quantum simulation.

The purpose of the present work is to study the effects of noise in an existing algorithm proposed for a quantum simulation and to take away from this example as much general understanding as we can. The primary noise considered is prior unknown correlations or entanglement within the system and between the simulated system and the environment. We study the evolution of different initial states, including ideal ones and states in which errors are present due to mistakes in preparation and/or interactions with particles in the system, and find the dynamical maps that represent the evolution. The algorithm we explore was proposed and developed by Ortiz *et al.* [6] to simulate the one-dimensional Fano-Anderson model. To examine various behaviors of the system with initial correlations, we first provide a background for the quantum simulation in Sec. I A, which focuses on the different sources of noise that can affect the experiments. Section I B provides a brief review of open system quantum dynamics and discusses dynamical maps and their main characteristics, including requirements for positivity and complete positivity; the purpose is to use dynamical maps to describe general errors in simulations. Section II contains a brief explanation of the algorithm used, including the modifications we made to represent noise in the system. Finally, our results, given in Sec. IV, are divided in two parts: those states for which the Bloch vector has a component only along the z direction, and those which have some small component along x and a main one along z. We will also discuss why this is important. These two last subsections are subsequently divided into simulations performed with no external noise and simulations carried out in the presence of noise. For the purpose of comparison, the

parameters of the system were obtained from Ref. [6] and were used for all the considered scenarios.

A. Quantum simulations

There are two main classifications of quantum simulators. The universal quantum simulator (UQS) [51] (also referred to as digital [52]), i.e., a quantum computer, represented by the standard circuit model given the set of universal gates that act on a collection of two-state systems [23,53,54]. The term *universal* infers that the quantum computer would be able to simulate any arbitrary quantum system [55,56], which implies universal quantum computation is possible. A universal quantum computer would be Lloyd's idea of a universal quantum simulator [56]. However, this device has not been built yet. So researchers have designed and implemented devices consisting of smaller, but controllable, quantum systems specifically intended to represent other quantum systems. These constitute the second type of quantum simulators, called specialized quantum simulators (SQSs) [51,57] or analog quantum simulators [52,58]. The latter are not intended for quantum computation nor as a universal simulator. Rather, they are able to simulate a smaller but interesting class of physical models. Quantum evolution in these systems is not necessarily carried out through a Trotter decomposition nor quantum gates; instead, they operate continuously in time subject to external controls [56]. Many interesting advances and simple simulations have already been performed using these specialized systems [16,18,39,44,45,47–49,59–62] examples of which include ultracold atoms, ion traps, quantum dots, atoms in optical lattices, coupled cavities, photons, electrons floating on He films, and NMR devices among others [4,16,18,19,33,45,46,50,52,60,63]. Although the above-mentioned are the two predominant classifications, there exists the possibility of a nonuniversal digital quantum simulator and a universal analog quantum simulator. The nonuniversal digital simulator, or special purpose quantum computer, would carry the Hamiltonian evolution through a Trotter decomposition but does not require a universal set of gates and therefore error correction and fault-tolerant operation are not guaranteed [56]. On the other hand, the universal analog simulator would not be subject to Trotterization but would be a system capable of simulating any other quantum system. A universal set of controls is not yet available for this kind of device [56]. Further details on these classifications can be found in Ref. [56].

Quantum simulators are open systems that are subject to unwanted interactions with an environment that can have a detrimental effect on the outcome. One may suppose that error correction and/or prevention can be used for accurate implementation, but the traditional methods will often not apply to SQSs [56]. Inaccurate unitary transformations are potential sources of noise as well, since they can affect the outcome of the experiment [6]. Therefore, having precise control over the system is the main problem of interest when performing a quantum simulation [3,64].

All steps, preparation, evolution, and measurement, can cause some degree of error [6,17] as well as unwanted interactions with other particles in the simulator, etc. It was initially suggested that decoherence in quantum simulations may not need to be treated in the same strict sense as in quantum computation [2], because noise in the simulating device might be able to be identified with noise in the simulated system. Nevertheless, the nature of the interactions of the simulator with the bath may not be the same as those of the system of interest and thus error prevention techniques of some sort will almost certainly be required. These include error-correcting codes (QECC) [65–70], decoherence-free subspaces and noiseless subsystems (DNS) [71–76] (see also [77,78] for reviews), and/or dynamical decoupling (DD) [63,79–89]. However, even if error correction is available, it means an increase in resource requirements and can represent a problem with scalability [3,4,58,90,91] and efficiency. There exist algorithms and observables which have an inherent robustness to errors [92], but this is not the case for all systems and all errors.

One may also attempt to simulate the interactions of a quantum system with a specific reservoir. Refs. [34,40,93] propose the simulation of systems that interact with an engineered bath that is modelled using other components in the quantum simulator (ancilla qubits in [40,93] and *LC* resonators in [34]). In Refs. [34,40] the experiments are proposed in order to simulate both, Markovian and non-Markovian dynamics. Furthermore, an experimental setup to study open system dynamics is proposed in [18]. It includes qubits that are prepared to represent the system and other qubits to represent the environment. In this way noisy preparation of states and operations can be implemented. These kinds of setups can be included in the classification *open system quantum simulators*, also provided in [56]. The form in which the evolution of the system is carried out would determine whether the simulator is digital or analog. The final state of the system in these types of devices can be determined by tracing out environmental degrees of freedom, thus obtaining the evolution under noisy gates or controls. In the Markovian regime this would correspond to nonunitary Lindblad operators [56]. It is noteworthy that the bath is also part of the simulator in the above-mentioned references. This does not guarantee that the simulation is not subject to imperfect controls and/or noise otherwise not taken into account. For example, the modeling of the environment could be imperfect.

Previous research aimed at understanding the effects of noise and errors in quantum simulations includes the work by Dür *et al.*, who propose an algorithm to generate many-body interactions from two-body interaction Hamiltonians [94] and study the influence of noise due to timing errors and two-body interactions in the Markovian regime and suggest methods to reduce its influence. Ajoy *et al.* study the effects of imperfect couplings on the simulation of a state transfer through a spin chain and find that the final state presents phase errors when the above-mentioned parameters deviate from their ideal values [42].

Our work examines primarily unwanted interactions within the system. We use an existing algorithm developed by Ortiz *et al.* in [6] which was originally proposed without considering possible errors in the implementation. We focus on improper preparation of the initial state and couplings to other particles within the system. There is no question that the initial state is important because the outcome of the simulation depends on it. A factor to consider is when errors are caused by

initial entanglement; because dynamical decoupling cannot remove those errors, since these controls rely on local unitary transformations to eliminate Hamiltonian interactions with a bath. Local unitary controls cannot change the entanglement between the system and the bath.

Experimentally, it has been observed that two different state preparation methods may not yield the same result and can have a profound effect on the outcome [95]. We observe the characteristics of the dynamical map (which will be described in more detail in the next section) that describe the evolution of different initial states and determine their positivity or complete positivity. Until recently, discussions of the evolution of an open quantum system were limited to completely positive maps. However, work by Pechukas [96] and more recently, by Shaji and Sudarshan [97] have provided demonstrations that a map does not need be completely positive for the end result to represent a physical state. It fact, the map does not even need to be positive; it must only be positive on a given domain in order to possibly represent a physical mapping. In certain circumstances dynamical maps can provide information about correlations in the initial state of the system, which could provide useful information about the effects of noise and interactions in quantum simulations. Furthermore, there are many sets of operators in the operator-sum decomposition which give rise to the same map. This is true of completely positive maps [98,99] as well as maps which are not completely positive [100].

B. Noise in quantum systems, completely and non-completely positive maps

The density matrix, or density operator, represents our knowledge of the quantum state of a system. In general, any density operator must satisfy the following conditions in order to represent a physical state [101]:

$$\rho = \rho^{\dagger}, \quad \text{it is Hermitian,} \tag{1}$$

$$\rho \geqslant 0, \quad \text{it is positive semidefinite, i.e., its eigenvalues are non-negative,} \tag{2}$$

$$\mathrm{Tr}(\rho) = 1, \quad \text{it has trace 1, i.e., the sum of the probabilities is 1.} \tag{3}$$

The evolution of a closed system is described by a unitary transformation, as

$$\psi(t) = U(t)\psi(0),$$

where $U(t) = \exp(-iHt)$. It follows that

$$\rho(t) = U(t)\rho(0)U(t)^{\dagger}.$$

The density operator is often written as an expansion of pure states,

$$\rho = \sum_j p_j |j\rangle\langle j|,$$

where the p_j are the probabilities associated with each of the states $|j\rangle$. If one of the probabilities is equal to 1 and the rest are 0, then the state is pure. For two-state systems we can write the density operator in terms of the 2×2 unit matrix and the Pauli operators

$$\rho = \tfrac{1}{2}(\mathbb{1} + \vec{a} \cdot \vec{\sigma}),$$

where the coefficients a_i are the projections along the x, y, and z directions of the so-called Bloch vector. This provides a representation of the quantum state, which is a geometric representation of the states of the qubits in terms of a sphere with radius 1. (For higher-dimensional systems, this is referred to as the polarization vector, coherence vector, or generalized block vector. See [102–108] and references therein.) The magnitude of the Bloch vector is constrained by the condition $\sqrt{a_x^2 + a_y^2 + a_z^2} \leqslant 1$, and $|\vec{a}| = 1$ represents a pure state. Thus any state on the surface of the Bloch sphere is a pure state. A mixed state is represented by a vector with $|\vec{a}| < 1$. With this notation it is possible to have a visual representation of the quantum states at different times.

A system S that is coupled to an environment E with Hilbert spaces $\mathcal{H}_S$ and $\mathcal{H}_E$, respectively, can be considered a larger isolated system whose initial state is described by $\rho_{SE}(0)$. The time evolution of this system is then given by the joint evolution of the system and environment

$$\rho_{SE}(t) = U(t)\rho_{SE}(0)U(t)^{\dagger}.$$

We are often only interested in the evolution of the system, S. Tracing out the environmental degrees of freedom provides us with the reduced dynamics of the system

$$\rho_S(t) = \mathrm{Tr}_E[\rho_{SE}(t)] = \mathrm{Tr}_E[U_{SE}(t)\rho_{SE}(0)U_{SE}^{\dagger}].$$

Once we obtain the reduced dynamics of S, we can find the map that transforms the initial state $\rho(0)$ into the final state $\rho(t)$. To obtain the "dynamical map" it is convenient to write the $N \times N$ density operator ρ as a $N^2 \times 1$ column vector that is transformed into another $N^2 \times 1$ column vector through the $N^2 \times N^2$ supermatrix A,

$$\rho'_{r's'}(t) = A_{r's',rs}\rho_{rs}(0), \tag{4}$$

where A describes the most general evolution of ρ [109]. In matrix notation

$$\rho' = A\rho. \tag{5}$$

Because ρ must be mapped to another positive ρ', the following conditions are imposed on A [101]:

$$A_{r's',rs} = (A_{s'r',sr})^*, \quad A \text{ preserves Hermiticity,} \tag{6}$$

$$\sum_{rsr's'} x_r^* x_s A_{rs,r's'} y_{r'}^* y_{s'} \geqslant 0, \quad A \text{ preserves positivity,} \tag{7}$$

$$\sum_r A_{rr,r's'} = \delta_{r's'}, \quad A \text{ is trace preserving.} \tag{8}$$

These conditions ensure that the conditions Eqs. (1)–(3) on the density operator are satisfied for the final state if they are satisfied for the initial state. The second condition implies that the eigenvalues of the final density operator are all non-negative. This condition is called the positivity condition and a map that satisfies this condition it is said to be positive.

By interchanging indices of A, we obtain another $N^2 \times N^2$ supermatrix B [101],

$$B_{rr',ss'} \equiv A_{rs,r's'}. \tag{9}$$

The $1 \times N^2$ rows of A become the $N \times N$ block matrices of B. The following conditions are imposed on B so that it represents a physical map:

$$B_{rr',ss'} = (B_{r'r,s's})^*, \quad B \text{ is Hermitian,} \tag{10}$$

$$\sum_{rsr's'} x_r^* y_{r'} B_{rr',ss'} x_s y_{s'}^* \geqslant 0, \quad B \text{ is positive semidefinite,} \tag{11}$$

$$\sum_r B_{rr',rs'} = \delta_{r's'}, \quad B \text{ is trace preserving.} \tag{12}$$

From these we may write

$$\rho(t) = B[\rho(0)]. \tag{13}$$

If B is decomposed into its eigenvectors and eigenvalues, the action of the map can be represented as follows:

$$B[\rho(0)] = \sum_\alpha \lambda_\alpha \zeta_\alpha \rho(0) \zeta_\alpha^\dagger,$$

where $\lambda_\alpha \in \mathbb{R}$ are the eigenvalues. The Hermiticity of ρ' is guaranteed by the restriction given in Eq. (10) [109], so that B must be Hermitian. The matrix A is required to transform $\rho(0)$ into another Hermitian state $\rho(t)$, but A is not necessarily Hermitian itself. The final state will be positive. When all of the eigenvalues of B are positive, the map is said to be a completely positive map. (See Ref. [110] and references therein.) If B has a negative eigenvalue but still transforms any positive $\rho(0)$ into a positive $\rho(t)$, then B is a positive but not a completely positive map.

Noncompletely positive (NCP) maps have been measured using quantum process tomography (QPT) [111,112], which has caused the specifics of QPT to be questioned [113]. But the possibility that a map which is not a completely positive map can transform a valid quantum state into another valid state has brought a great deal of interest in studying the conditions for complete positivity. This is in addition to the interest in NCP maps due to the partial transpose as an indicator of entanglement [114,115].

In 1994, Pechukas showed that complete positivity constrains a system to product states of the form $\rho_{SE} = \rho_S \otimes \rho_E$, where ρ_E is a fixed state of the bath [96,116], which excludes correlations and therefore excludes many physical situations. Alicki in Ref. [117] argued that there is no general definition for the reduced quantum dynamics beyond the weak coupling regime; therefore, when the system is in an initially correlated state with the environment, linear assignment maps have no unique definition [113], and linearity would only be preserved for states that are invariant under the transformation [117]. Pechukas replied in Ref. [116] and agreed that open system reduced dynamics can be nonlinear. However, Rodriguez-Rosario *et al.* examine the assignment maps and argue against giving up linearity by noting that the assignment maps can be linear if the conditions of consistency or positivity are relaxed, and favor relaxing the positivity condition [113]. A quantum system that interacts with the environment before our prescribed $t = 0$ can be described by completely positive dynamics if the environment does not re-act on the system [109], i.e., the coupling is weak and/or the initial state is in a particular form [96].

As mentioned above, when the map is completely positive, the eigenvalues of B in Eq. (13) can be taken to all be positive. When they are, Eq. (13) can be rewritten as

$$\rho(t) = B[\rho(0)] = \sum_\alpha \lambda_\alpha \zeta_\alpha \rho(0) \zeta_\alpha^\dagger = \sum_\alpha C_\alpha \rho(0) C_\alpha^\dagger, \tag{14}$$

where $C_\alpha = \sqrt{\lambda_\alpha}\zeta_\alpha$. Equation (14) is sometimes known as the Kraus representation or operator-sum decomposition [118], although it was originally discussed in this context by Sudarshan *et al.* [101]. Jordan *et al.* demonstrated that entanglement in the initial state of the system can lead to noncompletely positive maps that still transform a positive ρ into another positive ρ' [119]. Rodriguez-Rosario *et al.* found that for purely classical correlations, the "quantum discord" (defined below) vanishes, and this is a sufficient condition for completely positive reduced dynamics [120]. Later, Shabani and Lidar demonstrated that the quantum discord was also a necessary condition for complete positivity [121]. Quantum discord was introduced by Ollivier and Zurek in 2001, it is defined as a "measure of the quantumness of the correlations" [122] and is calculated as follows:

$$\delta(S:E) = H(E) - H(S,E) + H\left(S|\left\{\Pi_j^E\right\}\right), \tag{15}$$

$H(x) = H(\rho_x) = \mathrm{Tr}[\rho_x \log_d(\rho_x)]$ is the Von Neumann entropy, where d is the base of the logarithm, specified by the dimension of the system. And $H(S|\{(\Pi_j^E\})$ is the conditional entropy, defined as the entropy of the system with respect to a set of projective measurements performed on the environment. Quantum discord provides a measure of the nature of correlations; it vanishes for classical correlations and is maximum when there is entanglement.

II. BACKGROUND

As mentioned before, the extent to which the noise from the environment can be included in a quantum simulation is dependent on both the simulating and simulated systems. Of course, it would useful to have some previous knowledge of the system-bath interactions. However, this is often not the case. Here we study the effects of unwanted noise in a quantum simulation using an algorithm that simulates the one-dimensional Fano-Anderson model. In this case we have a realistic model of the interaction and use the dynamical maps of the system to describe the noisy evolution. Starting with different initial states of the system and bath, we reduce the dynamics to a two-particle model system. The algorithm requires the two particles to be initialized in a particular state. Due to interactions with external qubits in the simulating device, these initial conditions may be imperfect. In addition, if the particles are allowed to interact for some small time before the beginning of the actual algorithm, the particles could begin in a correlated or entangled state. We consider the possibility of errors in the preparation of one of the particles in the system as well as the possibility of correlations between particles. We added a visualization of the evolution of the Bloch vector in order to provide an intuitive picture of the differences in the initial states and how they evolve. It is useful to note that, regardless of the noncomplete positivity

of some of the maps obtained, the final state is a physical state and the system is a realistic physical model with realistic couplings. The significance of these results will be discussed in the conclusions. We now describe our methods and results.

A. Quantum algorithm

Negrevergne *et al.* proposed an algorithm for the quantum simulation of the one-dimensional Fano-Anderson model [15]. This model consists of an impurity described by an energy ϵ surrounded by a ring of n spinless fermions having energies ε_{k_i}. The fermions interact with the impurity, which is also a spinless fermion, through a hopping potential V [6,15]. The diagonalized wave-number representation of the Fano-Anderson Hamiltonian is given by [6,15]

$$H = \sum_{i=0}^{n} \varepsilon_{k_i} c_{k_i}^{\dagger} c_{k_i} + \epsilon b^{\dagger} b + V \sum_{i=0}^{n-1} (c_{k_i}^{\dagger} b + b^{\dagger} c_{k_i}) \delta_{k_i 0}. \quad (16)$$

The system is mapped via Jordan-Wigner transformation to the spin system to obtain [6]

$$\bar{H} = \frac{\epsilon}{2}\sigma_z^1 + \frac{\varepsilon_{k_0}}{2}\sigma_z^2 + \frac{V}{2}\left(\sigma_x^1\sigma_x^2 + \sigma_y^1\sigma_y^2\right). \quad (17)$$

Negrevergne *et al.* consider an NMR device for their simulation as do we, but the model is not limited to this type of device.

The simulator has an NMR drift Hamiltonian of the form [6]

$$H_d = \frac{1}{2}\left(\frac{(\epsilon + \varepsilon_{k_0})}{2} - \sqrt{\left(\frac{\epsilon - \varepsilon_{k_0}}{2}\right)^2 + V^2}\right)\sigma_z^1 + \frac{1}{2}\left(\frac{(\epsilon + \varepsilon_{k_0})}{2} + \sqrt{\left(\frac{\epsilon - \varepsilon_{k_0}}{2}\right)^2 + V^2}\right)\sigma_z^2. \quad (18)$$

The schematic representation of the system with two particles can bee seen in Fig. 1.

The control Hamiltonian for spins in the system is

$$H_c(t) = \sum_j \left[\alpha_{x_j}\sigma_x + \alpha_{y_j}\sigma_y\right] + \sum_{ij} \alpha_{i,j}\sigma_z^i\sigma_z^j, \quad (19)$$

where the α are controllable. The last term is considered controllable because it can be turned on and off with the x and y rotations.

To obtain the representation of the Hamiltonian in Eq. (17), the following control sequence can be applied to Eq. (18) [6]:

$$U = e^{i\frac{\pi}{4}\sigma_x^2} e^{-i\frac{\pi}{4}\sigma_y^1} e^{-i\frac{\theta}{2}\sigma_z^1\sigma_z^2} e^{i\frac{\pi}{4}\sigma_y^1} e^{i\frac{\pi}{4}\sigma_x^1} \times e^{-i\frac{\pi}{4}\sigma_x^2} e^{-i\frac{\pi}{4}\sigma_y^2} e^{i\frac{\theta}{2}\sigma_z^1\sigma_z^2} e^{-i\frac{\pi}{4}\sigma_x^1} e^{i\frac{\pi}{4}\sigma_y^2}. \quad (20)$$

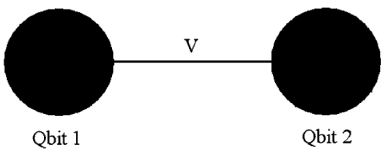

FIG. 1. Schematic representation of the simulated system. Qubit 1 is used to simulate the resonant impurity and qubit 2 represents a fermion site. The two particles interact via the potential V.

The goal is to see whether the initial state of the impurity has changed over time and, if so, how much. For this purpose, we use the time correlation function $C(t) = b(t)b(0)^{\dagger}$, which in spin operator representation becomes $C(t) = e^{i\bar{H}t}\sigma_-^1 e^{-i\bar{H}t}\sigma_+^1$ [6], where $\sigma_+ = \sigma_x + i\sigma_y$ and $\sigma_- = \sigma_x - i\sigma_y$. The time correlation function provides information about the overlap of the initial and final states of the impurity.

To study the behavior of this system, we will use the same form of the Hamiltonian in Eq. (17) to perform the unitary evolution on different initial states of the system, i.e., independent of any noise which may be present in the system. We perform the same operation regardless of prior interactions. We then obtain the reduced dynamics of the state of the impurity site (qubit 1) and then obtain the dynamical map that describes the evolution. We also calculate the time correlation function for the purpose of comparing the results of the different situations to those of an ideal scenario. In this way we observe the effects of the noise and possible errors in the outcome of the simulation.

B. Simulation with noise

To represent noise in the system, we include other qubits in the environment surrounding the system of interest and modify the control Hamiltonian. We examine two different models of noise:

(1) First, we added two spins and had them interacting via zz coupling with the particle that represents the state of the fermion site (see Fig. 2):

$$H_{\mathrm{NMR}} = \frac{1}{2}\left(\frac{(\epsilon + \varepsilon_{k_0})}{2} - \sqrt{\left(\frac{(\epsilon - \varepsilon_{k_0})}{2}\right)^2 + V^2}\right)\sigma_z^1 + \frac{1}{2}\left(\frac{(\epsilon + \varepsilon_{k_0})}{2} + \sqrt{\left(\frac{(\epsilon - \varepsilon_{k_0})}{2}\right)^2 + V^2}\right)\sigma_z^2 + \frac{J_{zz}}{4}\sigma_z^2\sigma_z^3 + \frac{J_{zz}}{4}\sigma_z^2\sigma_z^4 + \frac{J_{zz}}{4}\sigma_z^3\sigma_z^4. \quad (21)$$

(2) Next, we added an extra particle, which interacts in the same fashion (zz coupling) with both particles that represent the system of interest—the resonant impurity and the fermion

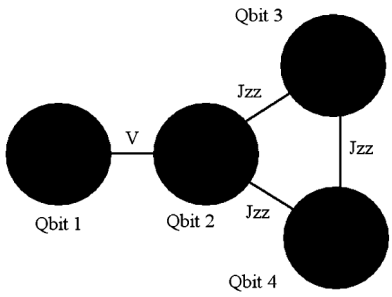

FIG. 2. Schematic representation of the simulated system. Qubit 1 is used to simulate the resonant impurity and Qubit 2 represents a fermion site. The two particles interact via the potential V. Qubit 2 interacts with two external spins (qubits 3 and 4) through the coupling term J_{zz}.

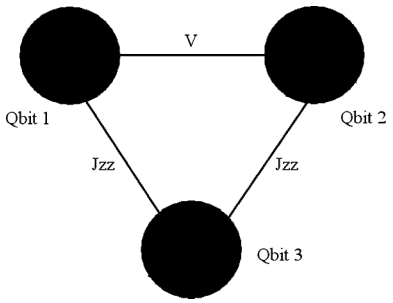

FIG. 3. Schematic representation of the simulated system. Qubit 1 is used to simulate the resonant impurity and qubit 2 represents a fermion site. The two particles interact via the potential V, and with an external spin (qubit 3) through the coupling term J_{zz}.

site (see Fig. 3):

$$H_{\mathrm{NMR}} = \frac{1}{2}\left(\frac{(\epsilon+\varepsilon_{k_0})}{2} - \sqrt{\left(\frac{(\epsilon-\varepsilon_{k_0})}{2}\right)^2 + V^2}\right)\sigma_z^1 + \frac{1}{2}\left(\frac{(\epsilon+\varepsilon_{k_0})}{2} + \sqrt{\left(\frac{(\epsilon-\varepsilon_{k_0})}{2}\right)^2 + V^2}\right)\sigma_z^2 + \frac{J_{zz}}{4}\sigma_z^1\sigma_z^3 + \frac{J_{zz}}{4}\sigma_z^2\sigma_z^3, \quad (22)$$

where J_{zz} represents the zz coupling constant. We used the same control sequence from Eq. (20) to obtain Eq. (17), to represent a situation in which the extra qubits are environmental. We therefore suppose these environmental spins are unknown and are only detectable through their effects on the system.

III. RESULTS

In this section we describe the results of the simulations for the two different modifications to the Hamiltonian as well as different initial states.

A. States with Bloch vector in the z direction

We first consider states with only a z component to their Bloch vectors. These form a special class of states due to the commutativity of the zz Hamiltonian with these initial states. This can be seen in Fig. 4, which represents the evolution of the Bloch vector at different times. The final state is spin directed along the z axis, but its magnitude changes in time.

1. Noiseless quantum simulation

Here we consider the cases where no bath is present but different initial states are considered. Three cases are considered, corresponding to three types of different initial states used in the simulation:

A.1 Pure states

$$|\psi(0)\rangle = |00\rangle, |01\rangle, |10\rangle, |11\rangle. \quad (23)$$

Density operator calculated as $\rho(0) = |\psi(0)\rangle\langle\psi(0)|$.

A.2 Entangled states

$$|\psi(0)\rangle = \alpha_0|01\rangle + \alpha_1|10\rangle, \quad (24)$$

where $\alpha_0^2 + \alpha_1^2 = 1$, and the density operator is given by $\rho(0) = |\psi(0)\rangle\langle\psi(0)|$.

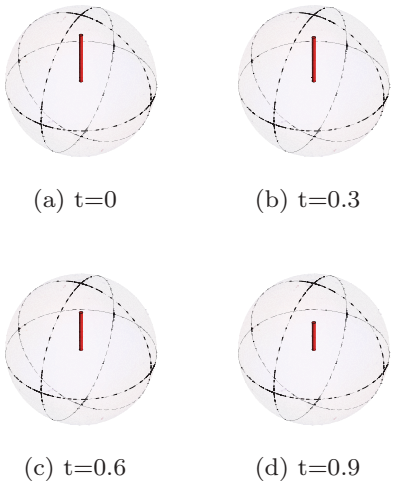

(a) t=0 (b) t=0.3

(c) t=0.6 (d) t=0.9

FIG. 4. (Color online) Evolution of the Bloch vector of the reduced dynamics of qubit 1 in the initial state $\rho_1 = |0\rangle\langle 0|$ as a function of time.

A.3 Correlated states

$$\rho(0) = (1-p)\left(\rho_1^I \otimes \rho_2^I\right) + p\left(\rho_1^{II} \otimes \rho_2^{II}\right), \quad (25)$$

where ρ_1^I and ρ_2^I are the density operators corresponding to some initial state of the impurity ("spin-down," occupied) and fermion ("spin-up," unoccupied), respectively, and ρ_1^{II} and ρ_2^{II} correspond to the other initial state of the impurity ("spin-up"/unoccupied) and fermion ("spin-up"/unoccupied).

We represented the initial state of the impurity in terms of its x, y, and z projections of the Bloch vector. The magnitude of each component of the projections a_i can be obtained by performing the partial trace over everything else except qubit 1, as $a_i = \mathrm{Tr}[\sigma_i(\rho_S(0))]$.

First consider an initial density operator

$$\rho_S(0) = \tfrac{1}{2}(\mathbb{1} + \vec{a}_i \cdot \vec{\sigma}_i).$$

In this case, case A.1,

$$\rho_S(0) = \tfrac{1}{2}(\mathbb{1} + a_3\sigma_z),$$

where a_3 represents a real constant that is equal to, or less than, the radius of the Bloch sphere (i.e., $0 \leqslant a_3 \leqslant 1$). It represents the projection along the z axis. The final state was obtained through the reduced dynamics of ρ_S after the evolution:

$$\rho_S(t) = \mathrm{Tr}\{\rho_S(0)[U(t)\rho(0)U(t)^\dagger]\}.$$

When the initial states $\rho_S(0)$ only had a z component, the final states $\rho_S(t)$ only had a z component as well:

$$\rho_S(t) = \tfrac{1}{2}(\mathbb{1} + b_3\sigma_z),$$

where b_3 is another real constant that is subject to $0 \leqslant b_3 \leqslant 1$. The value of b_3 depends on a_3 and on the parameters ϵ, ε_{k_i}, V, and t. When states with only a z component are input, the final states also have only a z component. This is consistent with the hopping model where the "spin-down" corresponds to the state being occupied. The evolution is described by the

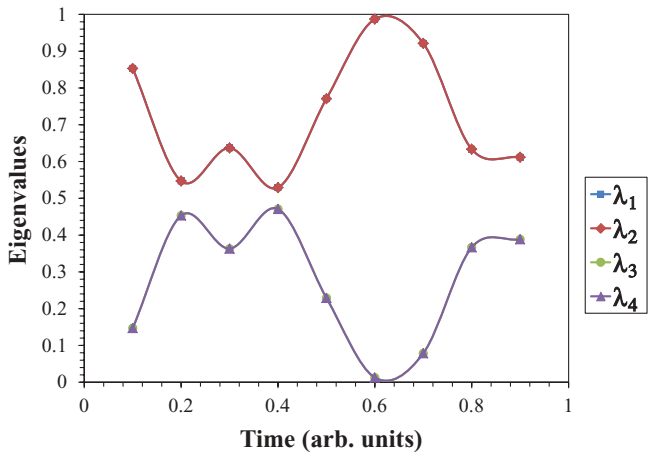

FIG. 5. (Color online) Eigenvalues of the dynamical map B of the reduced dynamics of qubit 1. The initial state of the *closed* system is $|\psi\rangle = |01\rangle$. This is an example of an initially pure state (case A.1) with zero quantum discord. The parameters of the Hamiltonian are $\epsilon = -8$ meV, $\varepsilon = -2$ meV, $V = 4$ meV. The evolution was carried out for the time interval $\Delta t \in [0.1, 0.9]$. There are four sets of eigenvalues, but due to the form of the dynamical map, two of these sets appear to overlap with the other two sets, which is the reason why only two lines show on the graph.

dynamical map

$$B = \begin{pmatrix} \frac{1+b_3}{2} & 0 & 0 & 0 \\ 0 & \frac{1+b_3}{2} & 0 & 0 \\ 0 & 0 & \frac{1-b_3}{2} & 0 \\ 0 & 0 & 0 & \frac{1-b_3}{2} \end{pmatrix}. \tag{26}$$

The eigenvalues of the map are plotted as functions of time in Fig. 5.

We note that the dynamical map for maximally entangled states (case A.2) in which only z components are considered for the initial states of both particles in the system has the same form as that in Eq. (26). In Fig. 5, the eigenvalues of the map correspond to a completely positive evolution. We found that this was the case for maximally entangled states with nonvanishing quantum discord, but only when the individual states of the particles are eigenvalues of the Fano-Anderson Hamiltonian. We found this to be the case for states of the form presented as case A.3 under the same conditions mentioned above.

We therefore note, for later reference, that in these cases all states have only a z component in the initial and final states of the system. Thus there is only this standard interpretation of the hopping model Hamiltonian when there is no external noise.

2. Simulation with noise from spin bath

In this section we present the results for systems governed by the Hamiltonians in Eqs. (21) and (22). The goal is to simulate a two-body problem, so we used the same control sequence in Eq. (20). However, the initial state of a "bath" of two particles was included in the total system Hamiltonian. As in the simulation that had no external noise, we chose different initial configurations. Explicitly, including the bath qubits these are:

A.4 Pure states

$$|\psi(0)\rangle = |0011\rangle, |0111\rangle, |1011\rangle, |1111\rangle, \tag{27}$$

and density operator $\rho(0) = |\psi(0)\rangle\langle\psi(0)|$.

A.5 Entangled states

$$|\psi(0)\rangle = \alpha_0|0111\rangle + \alpha_1|1011\rangle, \tag{28}$$

where $\alpha_0^2 + \alpha_1^2 = 1$, and the density operator is given by $\rho(0) = |\psi(0)\rangle\langle\psi(0)|$.

A.6 Correlated states

$$\rho(0) = \left[(1-p)\left(\rho_1^I \otimes \rho_2^I\right) + p\left(\rho_1^{II} \otimes \rho_2^{II}\right)\right] \otimes(|1\rangle\langle 1|) \otimes (|1\rangle\langle 1|). \tag{29}$$

The fact that the states only had a component in the z direction and only interact with the bath via zz couplings gives results very similar to the ones in the previous section. The initial state of qubit 1 (the impurity) can again be written in Pauli notation as

$$\rho_S(0) = \mathrm{Tr}_E \rho(0) = \tfrac{1}{2}(\mathbb{1} + a_3\sigma_z). \tag{30}$$

The final state is obtained by tracing over the bath degrees of freedom,

$$\rho_1(t) = \mathrm{Tr}_E[U(t)\rho(0)U(t)^\dagger] = \tfrac{1}{2}(\mathbb{1} + b_3\sigma_z), \tag{31}$$

where b_3 is another constant.

The most general dynamical map has the same form as the map in Eq. (26),

$$B = \begin{pmatrix} \frac{1+b_3}{2} & 0 & 0 & 0 \\ 0 & \frac{1+b_3}{2} & 0 & 0 \\ 0 & 0 & \frac{1-b_3}{2} & 0 \\ 0 & 0 & 0 & \frac{1-b_3}{2} \end{pmatrix}. \tag{32}$$

We observed that the coupling J_{zz} affects the rate of change of the state of qubit 1, which is shown in the results for the calculation of the time correlation function. In Figs. 6 and 7, the eigenvalues of B are plotted with the couplings to the particles of the spin bath being $J_{zz} = 8$ and $J_{zz} = \frac{1}{10}$, respectively.

Figures 5, 6, and 7 show the evolution of the same initial state, but each has a different environment. Being states initially in the z direction, the dynamics are completely positive since the interaction with the bath is a zz coupling. However, it does change the hopping rate. In Fig. 6 this is particularly noticeable due to the choice of the coupling. The state of the impurity does not transfer as quickly due to the strong correlations generated by the interaction with the spin bath. In Fig. 7 the situation is different. In this case the eigenvalues remained the same, regardless of the strength of the coupling with the environment. This is because the additional spin interacts with both particles in the system with the same coupling strength, producing an overall shift in the energy parameters of the system.

3. Weak, intermediate, and strong coupling regimes

The time for the transfer of the initial state of the system is clearly affected by the strength of the coupling. To better understand the effect of interactions with external spins, Fig. 8 represents the evolution of a state where both qubits 1 and 2 are initially aligned along the z axis. The "weak," "intermediate,"

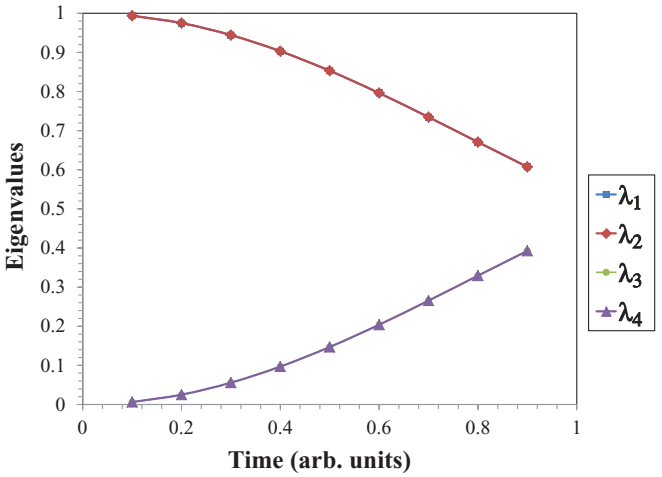

FIG. 6. (Color online) Eigenvalues of the dynamical map of the reduced dynamics of qubit 1. In the open system two qubits are interacting via zz coupling with qubit 2 with coupling constant $J_{zz} = 8$ meV. The initial state of the system and bath is given by $\psi = |0111\rangle$ (case A.4). The system parameters are $\epsilon = -8$ meV, $\varepsilon = -2$ meV, and $V = 4$ meV. The evolution is carried out for the time interval $t \in [0.1,0.9]$. The dynamical map of the reduced dynamics for this configuration is also completely positive. Similarly to the case of Fig. 5, there are two sets of eigenvalues which overlap.

and "strong," regimes are defined in terms of the strength of the coupling to the bath J_{zz} compared to the parameters of the system which were obtained from [6]. The coupling strength has an effect on the transfer rate. In the "strong" regime, where the coupling strength is larger than the parameters of the system, the evolution is much slower. The "weak" regime

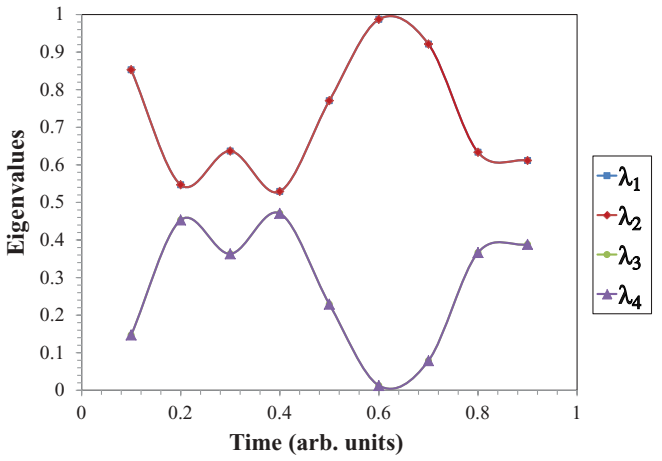

FIG. 7. (Color online) Eigenvalues of the dynamical map of the reduced dynamics of qubit 1. The system is open. An additional qubit is interacting via zz coupling with qubits 1 and 2 with coupling constant $J_{zz} = 1/10$ meV. The initial state of the system and bath is $|\psi\rangle = |011\rangle$ (case A.4 with only one additional qubit). The system parameters are $\epsilon = -8$ meV, $\varepsilon = -2$ meV, and $V = 4$ meV. The evolution is carried out for the time interval $t \in [0.1,0.9]$. This configuration was the same as in Fig. 5, because the couplings to the third qubit both had the same magnitude, which results in a shift in the values of the energies, but the relative sizes of the parameters remain unchanged.

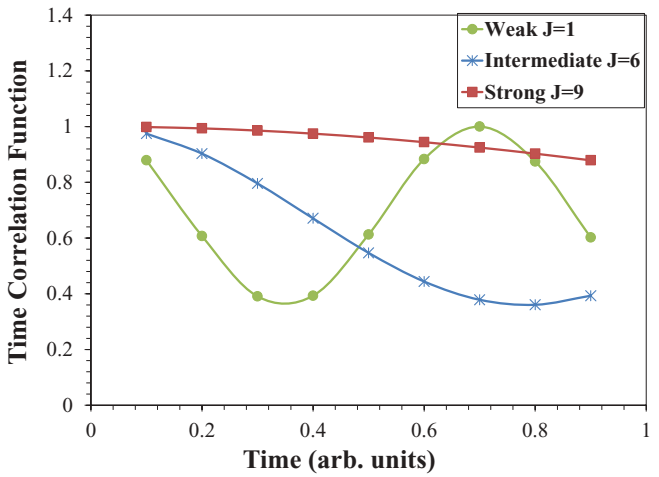

FIG. 8. (Color online) Time correlation function of the reduced dynamics of qubit 1. Qubit 2 is interacting via zz coupling with qubits 3 and 4. The coupling strengths are $J_{zz} = 1$ meV in the "weak" regime, $J_{zz} = 6$ meV in the "intermediate" regime, and $J_{zz} = 9$ meV in the "strong" regime. The initial state of the system and bath is $|\psi\rangle = |0111\rangle$ (case A.4). The system parameters are $\epsilon = -8$ meV, $\varepsilon = -2$ meV, and $V = 4$ meV, for times $t \in [0.1,0.9]$.

approximates the evolution of the system when no interaction with an external bath is present, thus making it more difficult to detect errors.

B. Arbitrary initial direction of the Bloch vector

Noise in the initialization of the state could result in a direction for the Bloch vector which is not in the z direction (see Fig. 9). States that have an x or a y component to their polarization vector, or Bloch vector, exhibit precession and approximate more accurately what happens in a real experimental situation. This is often observed in an NMR device under general circumstances and leads to noise in the system. Here we consider an initial state with a component of the Bloch vector in the x direction. Clearly a y component is not necessary and only specifies a different initial condition for the angle since the system will precess.

1. Noiseless quantum simulation

The initial states were chosen to have a component in the x direction; the components in x and z were selected such that the magnitude of the Bloch vector is close to 1, emulating a small error in the initialization. Explicitly, the different initial configurations were:

B.1 States in which qubit 1 has a component in the x direction

$$\rho_1(0) = \tfrac{1}{2}(\mathbb{1} + a_1\sigma_x + a_3\sigma_z)$$

and

$$\rho_2(0) = \tfrac{1}{2}(\mathbb{1} - \alpha_3\sigma_z).$$

B.2 Correlated states in which the initial state is a convex combination of states; one (or both) of the possible states of qubit 1 has a component in the x direction (state for qubit 1 in case B.1),

$$\rho(0) = \left[(1-p)\left(\rho_1^I \otimes \rho_2^I\right) + p\left(\rho_1^{II} \otimes \rho_2^{II}\right)\right],$$

where ρ_1 is the state of the impurity, ρ_2 is the state of the fermion and the a_i are subject to $0 \leqslant \sqrt{a_1^2 + a_3^2} \leqslant 1$.

The final state of the impurity was, once again, obtained by doing a partial trace over the degrees of freedom of the fermion

$$\rho(t) = \mathrm{Tr}_E[U\rho(0)U^\dagger] = \tfrac{1}{2}(\mathbb{1} + b_1\sigma_x + b_2\sigma_y + b_3\sigma_z). \quad (33)$$

The map B is given by

$$B = \begin{pmatrix} \frac{1+b_3}{2} & 0 & 0 & \frac{-ib_2}{a_1} \\ 0 & \frac{1+b_3}{2} & \frac{b_1}{a_1} & 0 \\ 0 & \frac{b_1}{a_1} & \frac{1-b_3}{2} & 0 \\ \frac{ib_2}{a_1} & 0 & 0 & \frac{1-b_3}{2} \end{pmatrix}. \quad (34)$$

The eigenvalues of B are given by

$$\lambda_1 = \frac{a_1 - \sqrt{4b_1^2 + a_1^2 b_3^2}}{2a_1}, \quad \lambda_2 = \frac{a_1 + \sqrt{4b_1^2 + a_1^2 b_3^2}}{2a_1}, \quad \lambda_3 = \frac{a_1 - \sqrt{4b_2^2 + a_1^2 b_3^2}}{2a_1}, \quad \lambda_4 = \frac{a_1 + \sqrt{4b_2^2 + a_1^2 b_3^2}}{2a_1}, \quad (35)$$

where

$$b_1 = \left\{ \cos\left(\frac{1}{2}t(\epsilon + \varepsilon_{k_0})\right) \cos\left(\frac{1}{2}t\sqrt{4V^2 + (\epsilon - \varepsilon_{k_0})^2}\right) - \sin\left(\frac{1}{2}t(\epsilon + \varepsilon_{k_0})\right)\left[\frac{(\epsilon - \varepsilon)\sin\left(\frac{1}{2}t\sqrt{4V^2 + (\epsilon - \varepsilon_{k_0})^2}\right)}{\sqrt{4V^2 + (\epsilon - \varepsilon_{k_0})^2}}\right]\right\} a_1,$$

$$b_2 = \left\{ -\sin\left(\frac{1}{2}t(\epsilon + \varepsilon_{k_0})\right) \cos\left(\frac{1}{2}t\sqrt{4V^2 + (\epsilon - \varepsilon_{k_0})^2}\right) - \cos\left(\frac{1}{2}t(\epsilon + \varepsilon_{k_0})\right)\left[\frac{(\epsilon - \varepsilon)\sin\left(\frac{1}{2}t\sqrt{4V^2 + (\epsilon - \varepsilon_{k_0})^2}\right)}{\sqrt{4V^2 + (\epsilon - \varepsilon_{k_0})^2}}\right]\right\} a_1$$

and

$$b_3 = \frac{2(-1 + a_3)V^2 + a_3(\epsilon - \varepsilon)^2 + (1 + a_3)V^2 \cos\left(\frac{1}{2}t\sqrt{4V^2 + (\epsilon - \varepsilon)^2}\right)}{4V^2 + (\epsilon - \varepsilon)^2}. \quad (36)$$

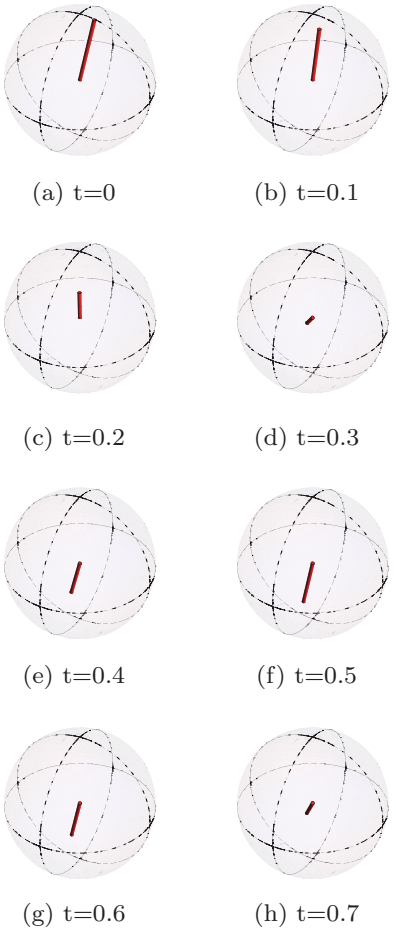

(a) t=0 (b) t=0.1 (c) t=0.2 (d) t=0.3 (e) t=0.4 (f) t=0.5 (g) t=0.6 (h) t=0.7

FIG. 9. (Color online) Animation of the evolution of the Bloch vector of the reduced dynamics of qubit 1 in the initial state $\rho_1 = \frac{1}{2}(\mathbb{1} + 0.2\sigma_x + 0.97\sigma_z)$.

Note that if $a_1 \mapsto 0$, then b_1 and b_2 are 0. The factor a_1 in the denominator of the eigenvalues is eliminated using l'Hospital's rule, and that yields

$$\lambda_1 = \frac{1 - b_3}{2}, \quad \lambda_2 = \frac{1 + b_3}{2}, \quad \lambda_3 = \frac{1 - b_3}{2}, \quad \lambda_4 = \frac{1 + b_3}{2}, \quad (37)$$

which are the same as the eigenvalues of the map in Eq. (26). The eigenvalues of B when $a_1 > 0$ are shown in Fig. 10. In Fig. 10, the dynamics of the system are positive but not

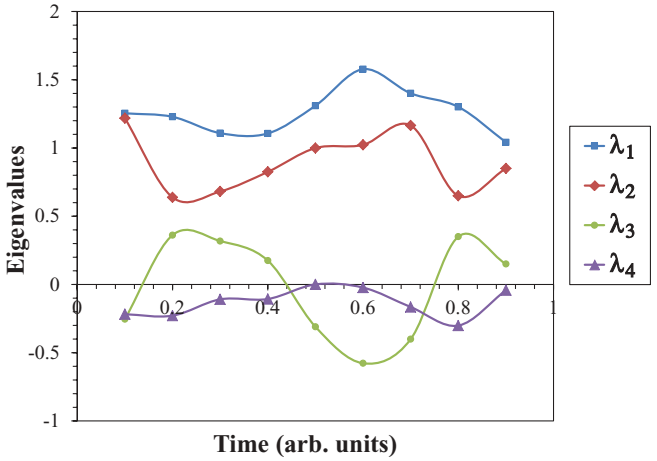

FIG. 10. (Color online) Eigenvalues of the dynamical map of the reduced dynamics of qubit 1. The initial states of the qubits in the closed system are $\rho_1 = \frac{1}{2}(\mathbb{1} + 0.2\sigma_x + 0.97\sigma_z)$ and $\rho_2 = \frac{1}{2}(\mathbb{1} - \sigma_z)$ (case B.1). The parameters of the Hamiltonian are $\epsilon = -8$ meV, $\varepsilon = -2$ meV, $V = 4$ meV. The evolution is carried out for the time interval $t \in [0.1, 0.9]$.

completely positive. This system is not in contact with a bath or reservoir, but it consists of two particles. This is a case of errors in initial state preparation. The general observation that can be made from these results is that when the initial state has a component of the Bloch vector in x or y as well as one in z, the result is an NCP map.

2. *Simulation with noise from the spin bath*

The results in this section are generated from adding the qubits in the spin bath and using the following initial states:

B.3 States in which qubit 1 has a component in the x direction in an open system,

$$\rho(0) = \rho_1(0) \otimes \rho_2(0) \otimes (|1\rangle\langle 1|) \otimes (|1\rangle\langle 1|), \tag{38}$$

where

$$\rho_1(0) = \tfrac{1}{2}(\mathbb{1} + a_1\sigma_x + a_3\sigma_z) \tag{39}$$

and

$$\rho_2(0) = \tfrac{1}{2}(\mathbb{1} - \alpha_3\sigma_z). \tag{40}$$

The reduced dynamics of S are given by

$$\rho(t) = \mathrm{Tr}_E[U(t)\rho(0)U(t)^\dagger] = \tfrac{1}{2}(\mathbb{1} + b_1\sigma_x + b_2\sigma_y + b_3\sigma_z), \tag{41}$$

with a B map of the same for as that in Eq. (34),

$$B = \begin{pmatrix} \frac{1+b_3}{2} & 0 & 0 & \frac{-ib_2}{a_1} \\ 0 & \frac{1+b_3}{2} & \frac{b_1}{a_1} & 0 \\ 0 & \frac{b_1}{a_1} & \frac{1-b_3}{2} & 0 \\ \frac{ib_2}{a_1} & 0 & 0 & \frac{1-b_3}{2} \end{pmatrix}. \tag{42}$$

Once again, the noise, which has the form of purely zz couplings, caused variations in the parameters, mostly in the rate of change of the state of qubit 1. The eigenvalues for a system with two spins interacting with the fermion only and for one spin interacting with both particles in the system are presented in Figs. 11 and 12.

In Figs. 11 and 12 the reduced dynamics are not completely positive. This is due to the initial state of the impurity site (qubit 1) having a component of its Bloch vector in the x direction. The algorithm was designed to have an initial state where one of the two state systems is in the up state and the rest are in the down state. Dynamical maps obtained through quantum process tomography can present discrepancies if the initial states are prepared through different experimental methods [95]. Thus the x component represents a preparation error which gives rise to an NCP map like in the previous case. Note that Fig. 12 is very similar to Fig. 10. In Fig. 12 the two qubits in the system are interacting with an external spin. Because, as mentioned before, this interaction is due to a zz coupling to the bath of the same strength for both particles, it represents only a shift in the energy parameters of the entire system. Therefore, the dynamics are the same in both cases. However, in Fig. 11 only qubit 2 is interacting with two external spins, and there is an effect on the eigenvalues of the dynamical map. The speed at which the system changes under the given Hamiltonian is affected; this can be verified with the time correlation function presented in the following section.

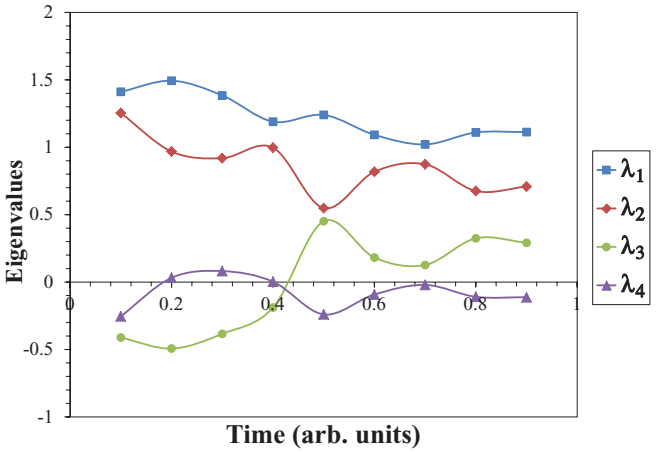

FIG. 11. (Color online) Eigenvalues of the dynamical map for the reduced dynamics of qubit 1. The initial states of the particles in the system are $\rho_1 = \frac{1}{2}(\mathbb{1} + 0.2\sigma_x + 0.97\sigma_z)$ and $\rho_2 = \frac{1}{2}(\mathbb{1} - \sigma_z)$. The initial states of the particles that compose the spin bath are $\rho_3 = \frac{1}{2}(\mathbb{1} - \sigma_z)$ and $\rho_4 = \frac{1}{2}(\mathbb{1} - \sigma_z)$. The total state of the bath is an example of case B.3. The Hamiltonian parameters are $\epsilon = -8$ meV, $\varepsilon = -2$ meV, $V = 4$ meV. The coupling to the bath has strength $J_{zz} = 6$ meV. The evolution is carried out in the time interval $t \in [0.1,0.9]$.

C. Time correlation function

Negrevergne *et al.* calculated the time correlation function $C(t) = b(t)b(0)^\dagger$ and plotted the result $|G|^2 = \mathrm{Tr}[\rho(t)\rho(0)]$ as a function of time. Since we want to calculate the effects of noise and different initial states, we followed the same procedure for the different situations. The results are summarized in the graphs of Figs. 13, 14, and 15. In Fig. 13, there is a slight difference between the results of the original system compared to those under which errors could arise

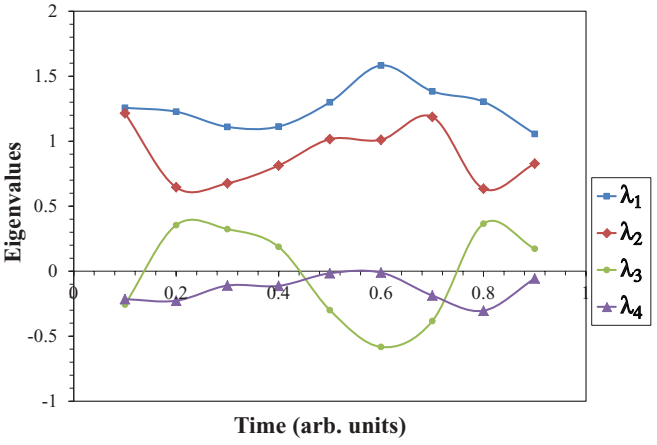

FIG. 12. (Color online) Eigenvalues of the dynamical map for the reduced dynamics of qubit 1. The initial states of the particles in the system are $\rho_1 = \frac{1}{2}(\mathbb{1} + 0.2\sigma_x + 0.97\sigma_z)$ and $\rho_2 = \frac{1}{2}(\mathbb{1} - \sigma_z)$. The initial state of the additional qubit is $\rho_3 = \frac{1}{2}(\mathbb{1} - \sigma_z)$. This is another form of case B.3, except that there is only one additional qubit acting as the bath. The Hamiltonian parameters are $\epsilon = -8$ meV, $\varepsilon = -2$ meV, $V = 4$ meV. The coupling to the additional qubit has strength $J_{zz} = \frac{1}{10}$ meV. The evolution of the system is evaluated for the time interval $t \in [0.1,0.9]$.

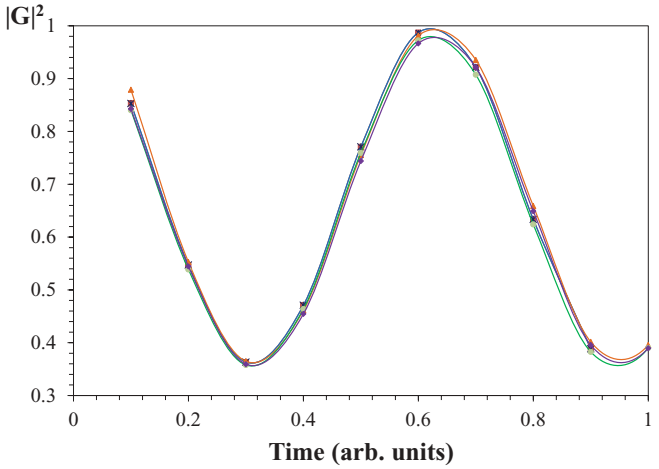

FIG. 13. (Color online) Time correlation function of the reduced dynamics of qubit 1. The Hamiltonian parameters are $\epsilon = -8$ meV, $\varepsilon = -2$ meV, $V = 4$ meV, for time interval $t \in [0.1,1]$. These results represent the evolution of the closed system, the system where qubit 2 interacts with two additional qubits, the system in which an additional qubit that interacts with qubits 1 and 2. This was done when qubit 1 was in the initial states $\rho = |0\rangle\langle 0|$ and $\rho = \frac{1}{2}(\mathbb{1} + 0.2\sigma_x + 0.97\sigma_z)$, as indicated above.

due to noise and unknown initial states. The coupling to the environment affects how fast or slow qubit 1 evolves. However, if the coupling to the bath is weak, these errors are not as prominent.

When the initial state had a component in x, the resulting correlation functions were very close to the original problem. This is important because a small error like this one may not be easily identified in the time correlation function. In Fig. 14 we show how the coupling to a spin bath can affect the rate of change of the evolution. As mentioned before, these results

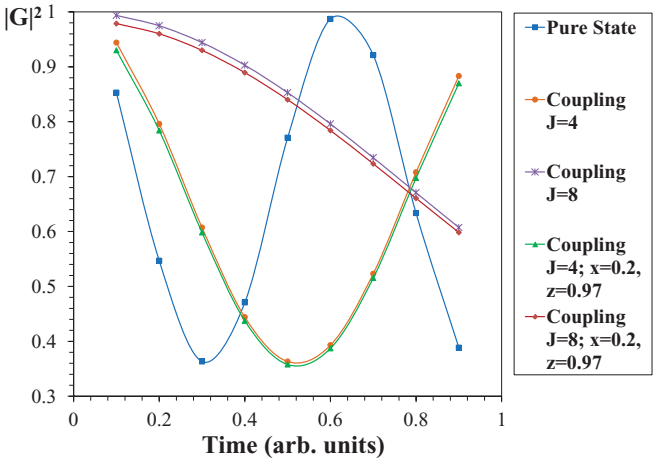

FIG. 14. (Color online) Time correlation function of the reduced dynamics of qubit 1. The system parameters are $\epsilon = -8$ meV, $\varepsilon = -2$ meV, $V = 4$ meV in the time interval $t \in [0.1,0.9]$. The results correspond to the closed system and the system that interacts with two additional qubits, coupled only to qubit 2. The initial state of qubit 1 is $\rho = |0\rangle\langle 0|$ for one set of results, and $\rho = \frac{1}{2}(\mathbb{1} + 0.2\sigma_x + 0.97\sigma_z)$ for the other.

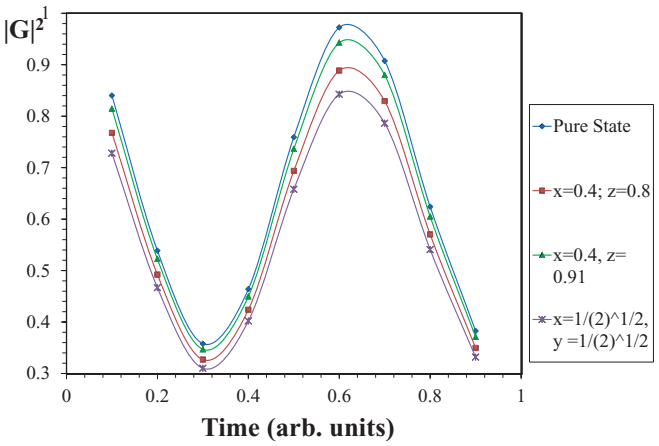

FIG. 15. (Color online) Time correlation function of the reduced dynamics of qubit 1. The system parameters are $\epsilon = -8$ meV, $\varepsilon = -2$ meV, $V = 4$ meV evaluated in the time interval $t \in [0.1,0.9]$. The result represents the time correlation function of the closed system compared to the correlation function of the reduced dynamics of qubit 1 in the initial state $\rho = \frac{1}{2}(\mathbb{1} + a_1\sigma_x + a_3\sigma_z)$ for different values of a_1 and a_3.

only include zz couplings. The strength of the couplings were adjusted in order to see the effects more clearly.

Because quantum simulations are performed on quantum systems, where access to complete information about the state at all times is not available, correlations with the bath can be by

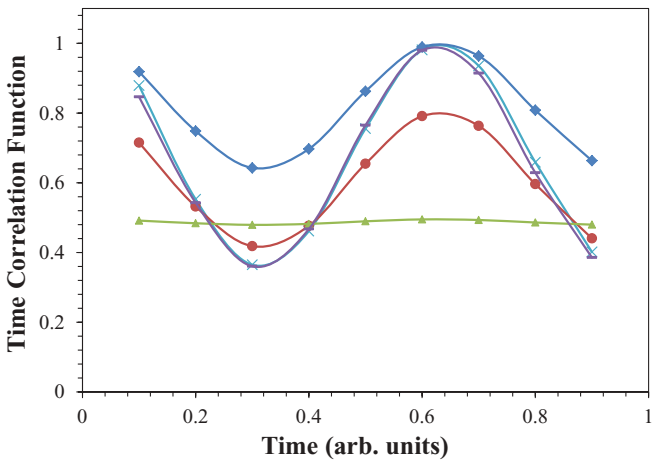

FIG. 16. (Color online) Time correlation function of the reduced dynamics of qubit 1. The system parameters are $\epsilon = -8$ meV, $\varepsilon = -2$ meV, $V = 4$ meV evaluated in the time interval $t \in [0.1,0.9]$. The results for the time correlation function of the reduced dynamics of qubit 1 for: a closed system where the two qubits are in a pure state (case A.1 label $\times$); a system where the initial state is a correlated one with $\rho_1^I = \frac{1}{2}(\mathbb{1} + 0.2\sigma_x + 0.97\sigma_z)$, $\rho_1^{II} = \frac{1}{2}(\mathbb{1} + \sigma_z)$, $\rho_2^I = \rho_2^{II} = \frac{1}{2}(\mathbb{1} - \sigma_z)$, and $p = \frac{1}{2}$ (case B.2 label $-$); a system where the initial state is a correlated one with $\rho_1^I = \frac{1}{2}(\mathbb{1} + 0.2\sigma_x + 0.97\sigma_z)$, $\rho_1^{II} = \frac{1}{2}(\mathbb{1} - 0.2\sigma_x - 0.97\sigma_z)$, $\rho_2^I = \frac{1}{2}(\mathbb{1} - \sigma_z)$, $\rho_2^{II} = \frac{1}{2}(\mathbb{1} + \sigma_z)$, and $p = \frac{1}{2}$ (case B.2 label $\triangle$); a system where the initial state is a correlated one (case A.3) where $\rho_1^I = \frac{1}{2}(\mathbb{1} + \sigma_z)$, $\rho_1^{II} = \frac{1}{2}(\mathbb{1} - \sigma_z)$, $\rho_2^I = \frac{1}{2}(\mathbb{1} - \sigma_z)$, $\rho_2^{II} = \frac{1}{2}(\mathbb{1} + \sigma_z)$, and $p = \frac{1}{9}$ ($\bigcirc$); a system where the initial state is a maximally entangled one (case A.5) and qubit 2 is interacting with two additional qubits with coupling strength $J_{zz} = \frac{1}{10}$ meV ($\Diamond$).

detected by differences in the rate of change of the evolution. In Fig. 15, we increased a_1, the component of the Bloch vector in x, to see how it affects the final result. When the x component of the Bloch vector is increased, we can see shifts in the time correlation function. The greater a_1 is, the larger the observed shift. This could be useful for detecting possible errors in state preparation.

In Fig. 16 we show the effects of initial correlations and entanglement on the time correlation function. When the initial state of the system is in the z direction, the maps are completely positive. However, the presence of entanglement and correlations is more evident in the time correlation function than a pure initial state. It is also more evident than in the case where the initial state has an x component. Maximally entangled states (case A.5) and correlated states exhibited the most pronounced deviations from the original results presented in Ref. [6]. Thus in an experiment, we expect these are more easily detected. However, deviations from complete positivity are not significantly reflected in the results. This leads us to believe that NCP maps which arise from small deviations in the initial preparation will not be easily detected.

IV. CONCLUSIONS

Interactions of quantum systems with a surrounding environment are undesirable for reliable quantum simulations and for quantum information processing in general. In order to enable the reduction or correction of noise, it is imperative that we try to understand and control or suppress the noise from the environment. Most research in error correction and fault tolerance has so far been devoted to universal quantum computing (and therefore universal quantum simulators) [56]. Lloyd's suggestion to *use* the noise to simulate the interaction of the system with the environment is clearly useful only in special cases. For some analog simulators, substantial isolation has been achieved [18]. However, noises remain in this system and in others.

It is known that interactions with the environment can lead to correlations that can result in noncompletely positive maps. We found that such maps are not rare in our study of a very simple model of a quantum system of fermions which can readily be simulated on a quantum computing device, or a dedicated quantum simulator. This Fano-Anderson model exhibits maps which are not completely positive for a variety of initial states, some of which were entangled and some with other nontrivial quantum correlations in the sense of nonzero quantum discord. They were shown to arise for even a fairly small transverse component to an initial density matrix which is supposed to have its Bloch vector aligned along the z axis. Thus fairly small experimental errors can lead to maps which are not completely positive in a rather simple experiment. These types of noise also cause relatively small errors in the final outcome of the measurement.

Initially correlated states, if they are not so identified but are instead identified improperly as arising from completely positive maps, may encourage an experimenter to try to employ dynamical decoupling controls to eliminate errors. These controls will be ineffective in these cases, since local unitary transformations will not remove initial correlations or entanglement.

We have used a very specific and simple model to illustrate the effects of noise on the system, including the presences of maps which are not completely positive. However, it is important to emphasize that these effects are quite general and will be present in some form in many other quantum systems, including a wide class of quantum simulations.

ACKNOWLEDGMENT

This material is based upon work supported by the National Science Foundation under Grant No. 0545798.

[1] R. P. Feynman, Int. J. Theor. Phys. **21**, 467 (1982).
[2] S. Lloyd, Science **273**, 1073 (1996).
[3] K. L. Brown, W. J. Munro, and V. M. Kendon, Entropy **12**, 2268 (2010).
[4] E. J. Pritchett, C. Benjamin, A. Galiautdinov, M. R. Geller, A. T. Sornborger, P. C. Stancil, and J. M. Martinis, arXiv:1008.0701v1.
[5] B. M. Boghosian and W. Taylor, Phys. Rev. E **57**, 54 (1998).
[6] G. Ortiz, J. E. Gubernatis, E. Knill, and R. Laflamme, Phys. Rev. A **64**, 022319 (2001).
[7] J. D. Biamonte, V. Bergholm, J. D. Whitfield, J. Fitzsimons, and A. Aspuru-Guzik, AIP Adv. **1**, 022126 (2011).
[8] S. Wiesner, arXiV:quant-ph/9603028.
[9] C. Zalka, Proc. Roy. Soc. London, Ser. A **454**, 313 (1998).
[10] R. Schack, Phys. Rev. A **57**, 1634 (1998).
[11] S. Somaroo, C. H. Tseng, T. F. Havel, R. Laflamme, and D. G. Cory, Phys. Rev. Lett. **82**, 5381 (1999).
[12] I. Kassal, S. P. Jordan, P. J. Love, M. Mohseni, and A. Aspuru-Guzik, Proc. Nat. Acad. Sci. USA **105**, 18681 (2008).
[13] R. Somma, G. Ortiz, J. E. Gubernatis, E. Knill, and R. Laflamme, Phys. Rev. A **65**, 042323 (2002).
[14] R. Somma, G. Ortiz, E. Knill, and J. Gubenartis, Int. J. Quantum Info. **1**, 189 (2003).
[15] C. Negrevergne, R. Somma, G. Ortiz, E. Knill, and R. Laflamme, Phys. Rev. A **71**, 032344 (2005).
[16] J. Simon, W. S. Bakr, R. Ma, M. E. Tai, P. M. Preiss, and M. Greiner, Nature (London) **472**, 307 (2011).
[17] C. R. Clark, T. S. Metodi, S. D. Gasster, and K. R. Brown, Phys. Rev. A **79**, 062314 (2009).
[18] J. T. Barreiro, M. Muller, P. Schindler, D. Nigg, T. Monz, M. Chwalla, M. Hennrich, C. F. Roos, P. Zoller, and R. Blatt, Nature (London) **470**, 486 (2011).
[19] K. R. Brown, C. Ospelkalus, A. C. Wilson, D. Leibfried, and D. J. Wineland, Nature (London) **471**, 196 (2011).
[20] S. Bravyi, D. P. DiVincenzo, D. Loss, and B. M. Terhal, Phys. Rev. Lett. **101**, 070503 (2008).
[21] S. P. Jordan, K. S. M. Lee, and J. Preskill, Science **336**, 1130 (2012).

[22] C. H. Bennett, J. I. Cirac, M. S. Leifer, D. W. Leung, N. Linden, S. Popescu, and G. Vidal, Phys. Rev. A **66**, 012305 (2002).

[23] J. L. Dodd, M. A. Nielsen, M. J. Bremner, and R. T. Thew, Phys. Rev. A **65**, 040301 (2002).

[24] P. Wocjan, M. Rotteler, D. Janzing, and T. Beth, Phys. Rev. A **65**, 042309 (2002).

[25] P. Wocjan, M. Roetteler, D. Janzing, and T. Beth, Quantum Inf. and Comput. **2**, 133 (2001).

[26] P. Wocjan, D. Janzing, and T. Beth, Quantum Inf. Comput. **2**, 117 (2002).

[27] M. A. Nielsen, M. J. Bremner, J. L. Dodd, A. M. Childs, and C. M. Dawson, Phys. Rev. A **66**, 022317 (2002).

[28] M. McKague, M. Mosca, and N. Gisin, Phys. Rev. Lett. **102**, 020505 (2009).

[29] A. M. Childs, E. Farhi, and J. Preskill, Quantum Inf. Comput. **10**, 669 (2010).

[30] A. M. Childs and R. Kothari, Quantum Inf. Comput. **10**, 669 (2010).

[31] A. M. Childs, D. Leung, L. Mancinska, and M. Ozols, Quantum Inf. Comput. **11**, 19 (2011).

[32] L.-A. Wu, M. S. Byrd, and D. A. Lidar, Phys. Rev. Lett. **89**, 057904 (2002).

[33] S. Mostame and R. Schutzhold, Phys. Rev. Lett. **101**, 220501 (2008).

[34] S. Mostame, P. Rebentrost, D. I. Tsomokos, and A. Aspuru-Guzik [New J. Phys. (to be published)].

[35] H. Wang, A. Aspuru-Guzik, and M. R. Hoffmann, Phys. Chem. Chem. Phys. **10**, 5388 (2008).

[36] J. D. Whitfield, J. Biamonte, and A. Aspuru-Guzik, Mol. Phys. **109**, 735 (2011).

[37] M.-H. Yung, D. Nagaj, J. D. Whitfield, and A. Aspuru-Guzik, Phys. Rev. A **82**, 060302 (2010).

[38] I. Kassal and A. Aspuru-Guzik, J. Chem. Phys. **131**, 224102 (2009).

[39] B. P. Lanyon, J. D. Whitfield, G. G. Gillett, M. E. Goggin, M. P. Almeida, I. Kassal, J. D. Biamonte, M. Mohseni, B. J. Powell, M. Barbieri, A. Aspuru-Guzik, and A. G. White, Nature (London) **2**, 106 (2010).

[40] H. Wang, S. Ashhab, and F. Nori, Phys. Rev. A **83**, 062317 (2011).

[41] K. L. Brown, S. De, V. M. Kendon, and W. J. Munro, New J. Phys. **13**, 095007 (2011).

[42] A. Ajoy, R. K. Rao, A. Kumar, and P. Rungta, Phys. Rev. A **85**, 030303 (2012).

[43] N. Wiebe, D. W. Berry, P. Hoyer, and B. C. Sanders, J. Phys. A **44**, 445308 (2011).

[44] J. Du, N. Xu, X. Peng, P. Wang, S. Wu, and D. Lu, Phys. Rev. Lett. **104**, 030502 (2010).

[45] X.-S. Ma, B. Dakic, W. Naylor, and P. Walther, Nature (London) **7**, 399 (2011).

[46] J. Cho, D. G. Angelakis, and S. Bose, Phys. Rev. A **78**, 062338 (2008).

[47] C. F. Roos, R. Gerritsma, G. Kirchmair, F. Zahringer, E. Solano, and R. Blatt, J. Phys.: Conf. Ser. **264**, 012020 (2011).

[48] R. Gerritsma, G. Kirchmair, F. Zahringer, E. Solano, R. Blatt, and C. F. Roos, Nature (London) **463**, 68 (2010).

[49] R. Gerritsma, B. P. Lanyon, G. Kirchmair, F. Zahringer, C. Hempel, J. Casanova, J. J. Garcia-Ripoll, E. Solano, R. Blatt, and C. F. Roos, Phys. Rev. Lett. **106**, 060503 (2011).

[50] M. Johanning, A. F. Baron, and C. Wunderlich, J. Phys. B **42**, 154009 (2009).

[51] I. Kassal, J. D. Whitfield, A. Perdomo, M. H. Yung, and A. Aspuru-Guzik, Annu. Rev. Phys. Chem. **62**, 185 (2011).

[52] I. Buluta and F. Nori, Science **326**, 108 (2009).

[53] D. Deutsch, Proc. R. Soc. London, Ser. A **400**, 97 (1985).

[54] V. Pavlov, *International Symposium on Modern Computing, 2006. JVA'06. IEEE John Vincent Atanasoff 2006* (IEEE, New York, 2006), pp. 235–239.

[55] C. H. Tseng, S. Somaroo, Y. Sharf, E. Knill, R. Laflamme, T. F. Havel, and D. G. Cory, Phys. Rev. A **61**, 012302 (1999).

[56] P. Hauke, F. M. Cucchietti, L. Tagliacozzo, I. Deutsch, and M. Lewenstein, Rep. Prog. Phys. **75**, 082401 (2012).

[57] M. A. Pravia, Z. Chen, J. Jepez, and D. G. Cory, Comput. Phys. Commun. **146**, 339 (2002).

[58] V. M. Kendon, K. Nemoto, and W. J. Munro, Phil. Trans. R. Soc. A **368**, 3609 (2010).

[59] E. Jane, G. Vidal, W. Dur, P. Zoller, and J. I. Cirac, Quantum Inf. Comput. **3**, 015 (2003).

[60] J. Zhang, G. L. Long, W. Zhang, Z. Deng, W. Liu, and Z. Lu, Phys. Rev. A **72**, 012331 (2005).

[61] P. Cappellaro, C. Ramanathan, and D. G. Cory, Phys. Rev. Lett. **99**, 250506 (2007).

[62] K. G. H. Vollbrecht and J. I. Cirac, Phys. Rev. A **79**, 042305 (2009).

[63] D. G. Cory, R. Laflamme, E. Knill, L. Viola, T. F. Havel, N. Boulant, G. Boutis, E. Fortunato, S. Lloyd, R. Martinez, C. Negrevergne, M. Pravia, Y. Sharf, G. Teklemariam, Y. S. Weinstein, and W. H. Zurek, Fortschr. Phys. **48**, 875 (2000).

[64] D. S. Abrams and S. Lloyd, Phys. Rev. Lett. **79**, 2586 (1997).

[65] P. W. Shor, Phys. Rev. A **52**, R2493 (1995).

[66] A. Steane, Rep. Prog. Phys. **61**, 117 (1998).

[67] A. R. Calderbank and P. W. Shor, Phys. Rev. A **54**, 1098 (1996).

[68] D. Gottesman, Phys. Rev. A **54**, 1862 (1996).

[69] D. Gottesman, Ph.D. thesis, California Institute of Technology, Pasadena, CA, 1997.

[70] F. Gaitan, *Quantum Error Correction and Fault Tolerant Quantum Computing* (CRC Press, Boca Raton, FL, 2008).

[71] P. Zanardi and M. Rasetti, Phys. Rev. Lett. **79**, 3306 (1997).

[72] D. A. Lidar, I. L. Chuang, and K. B. Whaley, Phys. Rev. Lett. **81**, 2594 (1998).

[73] L.-M. Duan and G.-C. Guo, Phys. Rev. A **57**, 737 (1998).

[74] E. Knill, R. Laflamme, and L. Viola, Phys. Rev. Lett. **84**, 2525 (2000).

[75] J. Kempe, D. Bacon, D. A. Lidar, and K. B. Whaley, Phys. Rev. A **63**, 042307 (2001).

[76] D. A. Lidar, D. Bacon, J. Kempe, and K. B. Whaley, Phys. Rev. A **63**, 022306 (2001).

[77] D. A. Lidar and K. B. Whaley, in *Irreversible Quantum Dynamics* (Springer-Verlag, Berlin, 2003).

[78] M. S. Byrd, L.-A. Wu, and D. A. Lidar, J. Mod. Opt. **51**, 2449 (2004).

[79] L. Viola and S. Lloyd, Phys. Rev. A **58**, 2733 (1998).

[80] M. Ban, J. Mod. Opt. **45**, 2315 (1998).

[81] L.-M. Duan and G. Guo, Phys. Lett. A **261**, 139 (1999).

[82] L. Viola, E. Knill, and S. Lloyd, Phys. Rev. Lett. **82**, 2417 (1999).

[83] P. Zanardi, Phys. Lett. A **258**, 77 (1999).

[84] D. Vitali and P. Tombesi, Phys. Rev. A **59**, 4178 (1999).

[85] L. Viola, S. Lloyd, and E. Knill, Phys. Rev. Lett. **83**, 4888 (1999).
[86] L. Viola, E. Knill, and S. Lloyd, Phys. Rev. Lett. **85**, 3520 (2000).
[87] D. Vitali and P. Tombesi, Phys. Rev. A **65**, 012305 (2001).
[88] M. S. Byrd and D. A. Lidar, Quant. Info. Proc. **1**, 19 (2001).
[89] G. S. Agarwal, M. O. Scully, and H. Walther, Phys. Rev. Lett. **86**, 4271 (2001).
[90] K. R. Brown, R. J. Clark, and I. L. Chuang, Phys. Rev. Lett. **97**, 050504 (2006).
[91] A. Papageorgiou and C. Zhang, Quantum Inf. and Comput. **11**, 541 (2012).
[92] L.-A. Wu and M. S. Byrd, Quantum Inf. Comput. **8**, 1 (2009).
[93] H. Weimer, M. Muller, and H. P. Buchler, Quantum Inf. Process. **10**, 885 (2011) .
[94] W. Dur, M. J. Bremner, and H. J. Briegel, Phys. Rev. A **78**, 052325 (2008).
[95] A.-M. Kuah, K. Modi, C. A. Rodríguez-Rosario, and E. C. G. Sudarshan, Phys. Rev. A **76**, 042113 (2007).
[96] P. Pechukas, Phys. Rev. Lett. **73**, 1060 (1994).
[97] A. Shaji and E. C. G. Sudarshan, Phys. Lett. A **341**, 48 (2005).
[98] M. A. Nielsen, C. M. Caves, B. Schumacher, and H. Barnum, Proc. R. Soc. London A **454**, 277 (1998).
[99] M. Nielsen and I. Chuang, *Quantum Computation and Quantum Information* (Cambridge University Press, Cambridge, UK, 2000).
[100] Y.-C. Ou and M. S. Byrd, Phys. Rev. A **82**, 022325 (2010).
[101] E. C. G. Sudarshan, P. M. Mathews, and J. Rau, Phys. Rev. **121**, 920 (1961).
[102] G. Mahler and V. A. Weberruss, *Quantum Networks: Dynamics of Open Nanostructures*, 2nd ed. (Springer Verlag, Berlin, 1998).
[103] Arvind, K. S. Mallesh, and N. Mukunda, J. Phys. A **30**, 2417 (1997).
[104] B.-G. Englert and N. Metwally, J. Mod. Opt. **47**, 2221 (2000).
[105] L. Jakóbczyk and M. Siennicki, Phys. Lett. A **286**, 383 (2001).
[106] M. S. Byrd and N. Khaneja, Phys. Rev. A **68**, 062322 (2003).
[107] G. Kimura, Phys. Lett. A **314**, 339 (2003).
[108] M. S. Byrd, C. A. Bishop, and Y.-C. Ou, Phys. Rev. A **83**, 012301 (2011).
[109] C. A. Rodriguez-Rosario and E. C. G. Sudarshan, Int. J. Quant. Inf. **9**, 1617 (2011).
[110] R. Horodecki, P. Horodecki, M. Horodecki, and K. Horodecki, Rev. Mod. Phys. **81**, 865 (2009).
[111] J. L. O'Brien, G. J. Pryde, A. Gilchrist, D. F. V. James, N. K. Langford, T. C. Ralph, and A. G. White, Phys. Rev. Lett. **93**, 080502 (2004).
[112] A. Bendersky, F. Pastawski, and J. P. Paz, Phys. Rev. Lett. **100**, 190403 (2008).
[113] C. A. Rodriguez-Rosario, K. Modi, and A. Aspuru-Guzik, Phys. Rev. A **81**, 012313 (2010).
[114] A. Peres, Phys. Rev. Lett. **77**, 1413 (1996).
[115] M. Horodecki, P. Horodecki, and R. Horodecki, Phys. Lett. A **223**, 1 (1996).
[116] R. Alicki, Phys. Rev. Lett. **75**, 3020 (1995); P. Pechukas, *ibid.* **75**, 3021 (1995).
[117] R. Alicki, Phys. Rev. Lett. **75**, 3020 (1995).
[118] D. M. Tong, L. C. Kwek, C. H. Oh, J.-L. Chen, and L. Ma, Phys. Rev. A **69**, 054102 (2004).
[119] T. F. Jordan, A. Shaji, and E. C. G. Sudarshan, Phys. Rev. A **70**, 052110 (2004).
[120] C. A. Rodriguez-Rosario, K. Modi, A.-M. Kuah, A. Shaji, and E. C. G. Sudarshan, J. Phys. A **41**, 205301 (2008).
[121] A. Shabani and D. A. Lidar, Phys. Rev. Lett. **102**, 100402 (2009).
[122] H. Ollivier and W. H. Zurek, Phys. Rev. Lett. **88**, 017901 (2001).